



Palaeoenvironmental conditions for the natural vulcanization of the Eocene “monkeyhair” laticifers from Geiseltal, Germany, as elucidated by Raman spectroscopy

Mara I. Lönart^{1,2} · Victoria E. McCoy^{3,4} · Carole T. Gee^{5,6} · Thorsten Geisler¹

Received: 13 June 2022 / Revised: 5 October 2022 / Accepted: 24 November 2022 / Published online: 28 February 2023

© The Author(s) 2023

Abstract

The evolutionary history of latex, a widespread chemical defense against insect herbivores, is not fully understood, yet a more detailed understanding of the fossil record of latex could help answer important evolutionary questions. This is, however, hampered by the difficulty of recognizing fossil latex and our still incomplete comprehension of the processes preserving latex. The best-studied fossil latex comes from the middle Eocene Geiseltal lignites in Germany, where fibrous laticifer mats, called “monkeyhair,” are preserved in the severely degraded remains of some ancient trees in the brown coals. Laticifers are specialized elongate cells that carry latex throughout the plant. In previous studies, researchers have hypothesized that these fossil laticifers are preserved through natural low temperature vulcanization of rubber within the latex. Here, we report the results of Raman spectroscopic study on Geiseltal laticifers to identify the vulcanization of natural rubber and on spatially associated carbonaceous material to test various Raman carbon geothermometers for their accuracy for low-thermal-maturity samples. Raman spectra of the fossil laticifers are virtually identical to that of rubber (*cis*-1,4-polyisoprene) with additional bands demonstrating sulfur vulcanization. Raman spectra from the surrounding lignite and existing Raman-based carbon thermometers, currently calibrated down to about 100 °C, clearly indicate that these samples were never exposed to temperatures higher than the surrounding lignite. These results directly validate the previous hypothesis of fossilization through natural vulcanization. Moreover, this work demonstrates that Raman spectroscopy is a rapid, non-destructive method for reliably identifying and characterizing fossil latex and that further development and calibration of the carbon thermometer may allow quantitative temperature measurements for low-thermal-maturity carbonaceous material.

Keywords Raman spectroscopy · Raman geothermometer · Natural vulcanization · Rubber · Fossil latex · Fossilization

Introduction

Latex is one of the most important and effective plant defenses against insect herbivores (Dussourd and Denno 1994;

Dussourd 2003, 2017; Hagel et al. 2008; Konno 2011). Latex commonly contains rubber, making it a sticky, viscous physical defense, as well as other bioactive compounds that come together to produce a complex chemical defense

✉ Mara I. Lönart
m.loenart@fz-juelich.de

Victoria E. McCoy
mccoyv@uwm.edu

Carole T. Gee
cgee@uni-bonn.de

Thorsten Geisler
tgeisler@uni-bonn.de

¹ Institute of Geoscience, Division of Geochemistry and Petrology, University of Bonn, Meckenheimer Allee 169, 53115 Bonn, Germany

² Present address: Institute of Energy and Climate Research (IEK-6): Nuclear Waste Management, Forschungszentrum Jülich GmbH, 52425 Jülich, Germany

³ Department of Geosciences, University of Wisconsin-Milwaukee, 3209 N. Maryland Avenue, Milwaukee, Wisconsin 53211, USA

⁴ Department of Geology, School of Geography, Geology, and the Environment, University of Leicester, University Road, Leicester LE1 7RH, UK

⁵ Institute of Geosciences, Division of Paleontology, University of Bonn, Nussallee 8, Bonn 53115, Germany

⁶ Huntington Botanical Gardens, 1151 Oxford Road, San Marino, California 91108, USA

(Konno, 2011). Latex and the related insect adaptations used to circumvent latex and effectively attack laticiferous plants are major components of plant–insect interactions in modern ecosystems (Agrawal and Konno 2009). However, little is known about the origin and evolutionary development of latex or about the role latex has played in ancient ecosystems. Notably, despite being one of the plant chemical defenses most commonly preserved in the fossil record (McCoy et al. 2021b; McCoy et al. 2022), little chemical study has been performed on fossil latex, with the exception of latex from the Geiseltal fossil site.

Fossil record of latex

Latex occurs in the palaeontological record starting in the latest Cretaceous and has been commonly reported in ancient members of the plant families Apocynaceae, Eucommiaceae, and Moraceae (McCoy et al. 2022). The best-studied and best-known fossil latex is fossilized rubber preserved in branched nonarticulated laticifers, which was originally called “*Affenhaar*” by German miners and in original German-language descriptions, or as “monkeyhair” in the more recent English translations, due to their stiff yet flexible, brown, hair-like appearance. Monkeyhair laticifers originate from the middle Eocene brown coals in the Geiseltal in Western Europe (Gothan 1924, 1927; Kindscher 1924; Jurasky 1928, 1930; Kirchheimer 1935; Krumbiegel et al. 1983; Mahlberg and Störr 1989; Wilde and Riegel 2010; McCoy et al. 2021a). These laticifers are unusual in that they are extremely common and are found as large, easily recognizable mats of fibers that are amenable to the destructive preparation of large samples for chemical analysis. Many of the earliest studies on the Geiseltal monkeyhair fossils noted that they were composed primarily of rubber (Gothan 1924, 1927; Kindscher 1924; Jurasky 1928, 1930), which was more recently confirmed and identified specifically as *cis*-1,4-polyisoprene, through IR analysis and solid state ^{13}C NMR (Beck-Mannagetta 1964; Mahlberg et al. 1984; Mahlberg and Störr 1989). As rubber is only naturally found in large quantities in latex, the last-cited set of results definitively identified the monkeyhair fossils as preserved latex.

In contrast to the Geiseltal monkeyhair fossils, other reported accounts of fossil latex—including reports of latex in fossil leaves from the Geiseltal, which has a different style of latex preservation than the monkeyhair fossils (McCoy et al. 2022)—are more commonly subtle laticifer strands or latex dots on fossil leaves, reproductive structures, or occur in silicified wood (e.g., Mathiesen 1975; Call and Dilcher 1997; McCoy et al. 2022, and references therein). The identification as fossil latex in these studies is solely based on morphology. This can be misleading, because some of these reports have been disputed, with the suggested latex dots re-interpreted as fungi (Kvaček and Sakala 1999) or as nondiagnostic, since it is

not always possible to distinguish laticifers from other secretory structures in fossils on the basis of morphology alone (Wilde et al. 2005; Franco 2010; Baas et al. 2017). Thus, the first hurdle in understanding the evolutionary history of latex is simply the correct recognition of fossil latex.

Fossilization of latex

The fossilization conditions that allow latex to preserve and any resulting biases that may influence our understanding of evolutionary patterns are also not yet fully understood, which is partly due to a lack of investigation into fossil laticiferous plants. The only research to date on latex fossilization has been carried out on the fossil monkeyhair laticifers from the Geiseltal. Extensive chemical analyses have strongly suggested, although not yet proven, that they were fossilized through natural vulcanization. Aside from the high rubber content in the fossil monkeyhair laticifers, it was also noted that they contain high concentrations of sulfur. The sulfur content and sulfur forms present were determined using controlled atmospheric programmed temperature oxidation and infrared sulfur analysis, indicating that the sulfur in the fossil laticifers is mostly organically bound and directly associated with the rubber (Mahlberg et al. 1984; Mahlberg and Störr 1989). The presence of rubber in association with high concentrations of organic sulfur, as well as the robustness of the fossil laticifers over geological time (Mahlberg et al. 1984; McCoy et al. 2021a), strongly suggests vulcanization, although it could also represent sulfur that is bound to the rubber without forming true cross links, or sulfur that is simply trapped in the rubber. This was further tested by the application of organic solvents (carbon disulfide, tetrahydrofuran, and chloroform) that can dissolve natural rubber but not vulcanized rubber, which failed to dissolve the fossil laticifers (Mahlberg et al. 1984). However, Mahlberg and Störr (1989) noted that the wood remnants surrounding the laticifers are also high in organically-bound sulfur, complicating the interpretation of exactly how sulfur is incorporated into the rubber and suggesting that more research is needed to determine if the sulfur forms true cross-links in the rubber.

Only about eight of 22 extant laticiferous families produce rubber in their latex (Hagel et al. 2008; Agrawal and Konno 2009; Konno 2011; Venkatachalam et al. 2013); all reports of fossil latex come from rubber-rich families (McCoy et al. 2022), suggesting that vulcanization of rubber may be the primary fossilization mechanism for latex. If further chemical analyses of other examples of fossil latex prove this to be the case, this would imply a major bias in the fossil record of latex, both towards plants with rubber-rich latex and also towards fossilization settings that allow for or even promote natural vulcanization.

Temperature may be one of the key environmental variables that influences vulcanization. Commercial vulcanization

of natural rubber is commonly carried out at temperatures between 140 – 180 °C, because it is at these high temperatures that vulcanization occurs more quickly and effectively (Mukhopadhyay et al. 1977; Mukhopadhyay and De 1979; Coran 1994; Joseph et al. 2015). Although it is still a matter of debate, it is assumed that sulfur reacts through radical mechanism with rubber chains to create sulfur cross-links of different length (mono-, di-, and polysulfide bonds), pendant side groups, and cyclic sulfides (Alliger and Sjothun 1964; Hofmann 1989). For sulfur vulcanization, activators (e.g., an activator complex constituted by an inorganic metal oxide such as ZnO) are used to increase the reaction efficiency of the vulcanization process (Hernández et al. 2016). At a fixed temperature of 170 °C, the progress of vulcanization or curing reaction can be monitored by Raman spectroscopy over the course of hours (Datta et al. 1999).

However, there is no evidence that the Geiseltal lignites as a whole were subjected to such high temperatures. In fact, the coals of Geiseltal are very immature according to a mean vitrinite reflectance value of $VR_o = 0.277\%$ which was determined from the coal of section G II in the adjacent Muehlen-Westfeld pit (Schmitz et al. 2001), classifying them as subbituminous and suggesting a peak burial temperature below about 60 °C (Burnham and Sweeney 1989; Barker and Goldstein 1990). A lack of charcoal also suggests that wildfires were rare (Wilde and Riegel 2010), making it unlikely that local heat production from fires could contribute to high-temperature vulcanization and leading some to suggest that the monkeyhair laticifers represent a natural example of low-temperature vulcanization (McCoy et al. 2021a). If other fossil latex is also vulcanized, however, this may occur at a range of temperatures.

Raman spectroscopy in the study of fossil latex

Here we apply *in situ* confocal Raman spectroscopy to fossil laticifers from the Geiseltal to answer some open questions about these fossils and to assess the utility of Raman spectroscopy for broader studies of fossil latex. Many other types of fossil latex occur in small amounts in rare fossils (McCoy et al. 2022), and so Raman spectroscopy with a micrometer-sized spatial resolution would be an ideal tool for non-destructive analysis *in situ* without high demands on sample preparation (e.g., Geisler and Menneken 2021).

Vulcanized rubber has a Raman spectrum distinct from that of natural rubber (Jackson et al. 1990; Hendra and Jackson 1994; Xue 1997; Samran et al. 2004; Taksapattanakul et al. 2017). Therefore, the analysis of monkeyhair laticifers could provide the first direct evidence that the Geiseltal laticifers are sulfur-vulcanized. In fact, as shown in the following, the Raman spectroscopic analyses of the Geiseltal monkeyhair laticifers demonstrate that Raman spectroscopy can identify rubber and its structural state in response to potential maturation processes in fossil material. Moreover, Raman spectroscopy

has been demonstrated to serve as a reliable tool to characterize the thermal maturity of carbonaceous matter on the micrometer scale which is reasonably well-constrained for thermally mature carbonaceous material that experienced temperatures higher than about 100 °C (e.g., Henry et al. 2019). Here we apply Raman spectroscopy to the carbonaceous material that partly coats the Geiseltal monkeyhair laticifers that is interpreted as degraded remains of wood or tree bark that once surrounded the laticifers (McCoy et al. 2021a) or as the cell walls of the laticifers themselves (Mahlberg et al. 1984). Based on the thermal history of the Geiseltal fossil site, these laticifers are known to have a low-thermal maturity. We also compare a variety of Raman spectroscopy geothermometry models to the Raman spectra from the bark to assess their usability for immature carbonaceous matter.

Geological and palaeontological background

The material under study here comes from the lignite deposits in the Geiseltal (Geisel Valley) in central Germany near the city of Halle an der Saale. The original deposits measured over 100 m thick and were commercially mined from the 17th century through 1992 (Eissmann 2002; Wilde and Riegel 2010). The lignites can be divided into three seams, the lower *Unterkohle*, the middle *Mittelkohle*, and the upper *Oberkohle*.

The Geiseltal site is generally well-known for its exceptionally preserved flora, which include trees containing laticifers, as well as a plethora of other plant remains, and a fauna of invertebrates and vertebrates (Krumbiegel 1959; Krumbiegel et al. 1983; Eissmann 2002). Isolated laticifers (the classic monkeyhair) are found at various intervals within the *Mittelkohle*, which exhibits poorer tissue preservation, such as the lack of preserved wood around the laticifers, than in the *Unterkohle* and *Oberkohle* (Wilde and Riegel 2010).

The laticiferous monkeyhair wood, *Coumoxylon hartigii*, has been assigned to the family Apocynaceae and is thought to resemble the extant genus *Couma* in its wood anatomy (Gottwald 1976). The well-preserved fossil remains analyzed by McCoy et al. (2021a) and investigated in the present study represent either the woody trunk of a small to medium-sized tree, or the woody branches of a large tree (McCoy et al. 2021a). The tree grew in a hot, humid, tropical to subtropical forest or peat bog during the middle Eocene (Riegel et al. 1999; Eissmann 2002; Wilde and Riegel 2010).

Materials and methods

Specimens

The fossil specimens analyzed in this study, inventory numbers GMH LIX20 and GMH Y74, are deposited in the Geiseltal Collections at the Martin-Luther-University in

Halle-Wittenberg, Germany. Monkeyhair fossils are typically mats of preserved laticifers without any associated tissue (Mahlberg et al. 1984; Mahlberg and Störr 1989; Wilde and Riegel 2010). However, the laticifer specimens selected for this study are remarkable as they are unusually well-preserved and still partially embedded in a degraded wood-like matrix. Furthermore, the surface of the laticifer mats of both specimens is still loosely attached to remnants of the tree bark (McCoy et al. 2021a). The laticifers were analyzed by Raman spectroscopy to assess if they are composed of vulcanized rubber (Fig. 1a, b). The surrounding carbonaceous material, remnants of either wood, bark, or laticifer cell walls, was analyzed to investigate the degree of maturation (Fig. 1b, c).

Raman spectroscopy

The Geiseltal laticifers were analyzed with a Horiba Scientific LabRam HR800 confocal Raman spectrometer, equipped with an Olympus BX41 microscope, located at the Institute of Geosciences, Division of Geochemistry and Petrology, at the University of Bonn, Germany. Raman scattering was excited with a HeNe laser (632.816 nm) with a power of less than 3 mW at the sample surface to avoid any sample heating. The scattered light was detected with an electron multiplier charge-coupled device (CCD) detector after having passed a 600 μm confocal aperture, a 100 μm spectrometer entrance slit, and being dispersed by a grating of 600 grooves/mm. Generally, spectra were recorded in the frequency range from 700 to 1800 cm^{-1} and 2600 to 3200 cm^{-1} with an exposure time of 25 to 30 s and 25 accumulations. In addition, few spots were measured in the frequency range from 250 to 700 cm^{-1} . Since the Raman signals from the laticifers in this frequency range are extremely weak and only a low laser intensity could be used, very long counting times of up to 90 accumulations of 60 s had to be used to obtain a sufficient signal-to-background ratio. The spectrometer was calibrated with spectral lines from a Ne lamp, the width

of which yielded an empirical spectral resolution between 3.3 and 3.0 cm^{-1} in the frequency range between 250 and 3200 cm^{-1} . All spectra were white-light corrected, i.e., corrected for the wavelength-dependence of the instrument sensitivity. The Raman spectra were then background-corrected using a 2nd order polynomial function within the measured frequency range. For the deconvolution and determination of the band frequency, Gauss-Lorentz functions were least-squares fitted to the measured spectra (cf., Supplement Fig S1). The background-uncorrected raw Raman spectra are given in addition in the Supplement (Fig S2).

Raman spectroscopic measurements of the brownish-black carbonaceous material matrix surrounding the laticifers were performed with a LabRAM HR Evolution UV-VIS system which is equipped with an open Olympus BX43 microscope. A Nd:YAG laser (532.09 nm) was used as excitation source. The laser power was set to $< \sim 3$ mW at the sample surface. Systematic test measurements with different laser power revealed that such a low laser energy was necessary to avoid any modification of the organic material through laser heating (cf. Henry et al., 2018). The acquisition time was 20 accumulations of 0.25 s per spot analysis. All other instrumental parameters were identical to those used with the LabRam HR800 spectrometer. To apply geothermometer models and determine which seemed the most promising for extension to low-maturity material, least-squares fitting of the Raman spectra was performed in accordance with the fitting procedures given by the respective authors (Rahl et al. 2005; Homma et al. 2015; Sauerer et al. 2017; Henry et al. 2019).

Results and discussion

Identification of vulcanized rubber in fossil latex

Figure 2 shows representative Raman spectra from the two sets of Eocene Geiseltal laticifers, specimens GMH LIX20

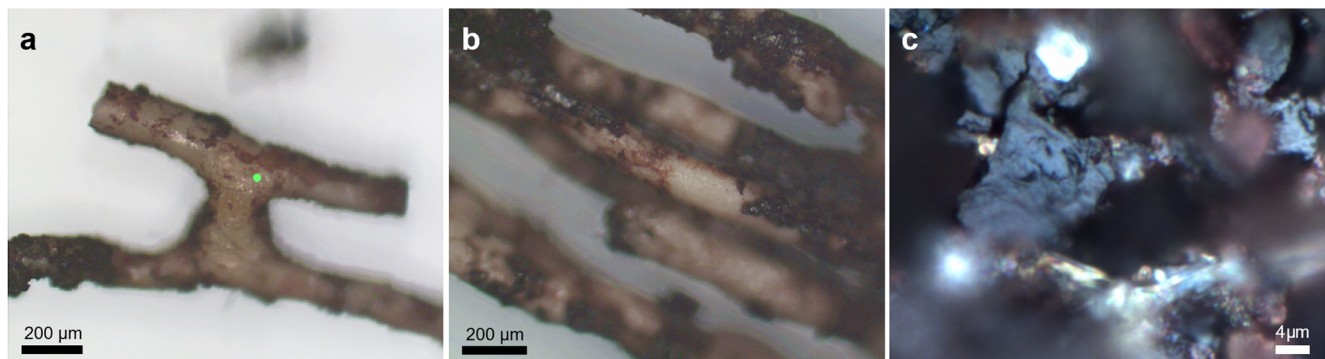


Fig. 1 **a** Well-preserved, branched laticifers from Geiseltal sample GMH Y74. The green dot marks the location of the upper Raman spectrum shown in Fig. 2. **b** Mat of the fiber-like laticifers from Geiseltal specimen GMH LIX20. Note that the brownish-blackish material

directly covers the laticifers and, in turn, is overlain by black carbonaceous material. **c** Black carbonaceous matrix of bark from specimen GMH Y74

and GMH Y74, respectively. A list with all observed frequencies is given in Table 1, along with the assignment of the observed bands to distinct molecular vibrations. The strong and relatively sharp Raman band at 1664 cm^{-1} corresponds to the $\nu(\text{C}=\text{C})$ stretching mode (Hendra and Jackson 1994; Koenig et al. 1971). The position of the $\nu(\text{C}=\text{C})$ at 1664 cm^{-1} is characteristic for the *cis*-1,4-polyisoprene of natural rubber. In contrast, this band is located at 1671 cm^{-1} for *trans*-1,4-polyisoprene (Haider 2012). The weak band at 1642 cm^{-1} is known to represent the $\nu(\text{C}=\text{C})$ vibrations of vinyl polyisoprene (Cornell and Koenig 1969; Datta et al. 1999), but was also observed in the Raman spectrum of *cis*-reference material investigated by Haider (2012). In line with this, Bunce et al. (1993) observed further characteristic frequencies at 1375, 1364, 1326, 1312, and 1287 cm^{-1} . All of these bands can also be identified in the Raman spectra obtained in this study (Fig. 2 and Table 1), suggesting the existence of natural rubber with *cis*-configuration. In the frequency region between 1415 and 1475 cm^{-1} , intense and overlapping bands near 1447 and 1439 cm^{-1} with shoulders at 1458 and 1432 cm^{-1} can be observed and attributed to the deformation $\delta(\text{CH}_2)$ modes which are also known as characteristic bands of the *cis*-1,4-isomers (Hendra and Jackson 1994; Nallasamy and Mohan 2004; Samran et al. 2004). However, a clear differentiation between the different isomers is difficult due to the broad nature of the Raman bands, which may hide further bands that may be related to vinyl units.

The Raman spectra from the fossil rubber differ from those of non-fossilized natural rubber by the presence of two additional intense bands near 1624 and 1594 cm^{-1} (Fig. 2). These bands are known to reflect sulfur vulcanization and are attributed to conjugated diene or conjugated undersaturated ($-\text{C}=\text{C}-\text{C}=\text{C}-$) species, indicative of main chain modifications and the destruction of sulfur crosslinks (Jackson et al. 1990; Hendra and Jackson, 1994; Xue 1997; Samran et al. 2004; Taksapattanakul et al. 2017). Hendra and Jackson (1994) observed bands near 1630 cm^{-1} , 1609 cm^{-1} , and 1591 cm^{-1} and assigned those bands to dialkenyl sulfide, a conjugated diene, and a conjugated triene species, respectively. In this and other studies (Xue 1997; Taksapattanakul et al. 2017), however, the band near 1609 cm^{-1} could not be deconvoluted successfully. The additional bands observed between 1590 and 1650 cm^{-1} assigned to the conjugated species show significant variations in the intensity relative to the stretching $\nu(\text{C}=\text{C})$ mode, reflected by significantly different ratios of the integrated intensity between 1480 and 1650 cm^{-1} and between 1650 and 1700 cm^{-1} (see values given in Fig. 2). These variations might indicate local differences in the main chain modification and thus local differences in the degree of vulcanization.

Beside the two characteristic bands of sulfur vulcanization (1594 and 1624 cm^{-1}), additional, yet unidentified bands are visible in the Raman spectra from the Geiseltal laticifers in the wavenumber region between 1480 and 1590 cm^{-1} (labeled 1

to 5 in Fig. 2 and Table 1). Previous chemical analyses suggested that some original latex compounds other than rubber are also preserved in the fossil laticifers that were possibly trapped within the vulcanized rubber. In particular, extracts analyzed by gas chromatography, gas–liquid chromatography, gas chromatography/mass spectrometry, and high-resolution mass spectrometry revealed various hydrocarbons, some of which were likely original components of the latex, while others may represent bacterial biomarkers produced during degradation of the monkeyhair tree (Mahlberg et al. 1984; Mahlberg and Störr 1989; Collins et al. 1995; Simoneit et al. 2003). It is thus tempting to relate the weak, yet unidentified Raman bands in the wavenumber region between 1480 and 1590 cm^{-1} to these other latex compounds.

In vulcanized natural rubber systems, poly- and disulfidic cross-links are expected to produce prominent bands in the region 400 – 550 cm^{-1} due to S–S stretching vibrations (Koenig et al. 1971; Hendra and Jackson 1994; Xue 1997; Hernández et al. 2016). In fact, a relatively intense but broad Raman profile is observed in the frequency region between 420 and 460 cm^{-1} , (inset of Fig. 2). The profile can be deconvoluted into three contributions at 421 cm^{-1} , 434 cm^{-1} , and 451 cm^{-1} (Table 1, Supplement Fig. S1A) which can be assigned to S–S stretching vibrations of ethyl sulfide units (Koenig et al. 1971), supporting the existence of $\nu(\text{S}-\text{S})$ stretching modes. However, the band near 421 cm^{-1} may also be assigned to the $\gamma(=\text{C}-\text{C}_2)$ rocking mode (Table 1).

Xue (1997) suggests that polysulfidic bonds are formed at the beginning of the vulcanization process, which then break down into mono- and disulfidic crosslinks during the course of the hardening process. In a more recent study from Hernández et al. (2016), the broad band around 500 cm^{-1} was deconvoluted into two bands near $\sim 488\text{ cm}^{-1}$ and $\sim 505\text{ cm}^{-1}$ and assigned to di- and polysulfide linkages, respectively, to quantitatively determine the types of S–S bridges present in different rubber formulations as a function of the hardening time and sulfur content. At the same time, Hernández et al. (2016) strongly emphasize that the analysis of this frequency region is non-trivial due to overlapping bands that are affected by different S–S linkages. In the spectrum of the GMH LIX20 specimen, a splitting of this band into two bands at 491 cm^{-1} and 505 cm^{-1} is clearly observed, correspondingly assigned to the disulfide and polysulfide species (inset in Fig. 2 and Table 1, Supplement Fig. S1A). Although the observed bands point to the presence of sulfide species, it must be considered that in the same region bending $\delta(\text{C}-\text{C})$ modes can also occur that are linked to non-vulcanized *cis*-polyisoprene (Cornell and Koenig 1969; Haider 2012).

Relative intense bands are located between 550 and 600 cm^{-1} which cannot be assigned at this time (labeled 6 to 9 in the inset of Fig. 2 and Table 1). These unassigned Raman bands, however, may also reflect the occurrence of other latex compounds, as bands 1 to 5 do. A relatively pronounced band

Table 1 Raman band frequencies (cm⁻¹) measured in Eocene laticifers from Geiseltal and their assignments to distinct vibrational modes if known

This study	No. (Fig. 2)	Assignment	References
2965		$\nu(\text{C}=\text{C}-\text{H})$	Cornell and Koenig (1969)
2935		$\nu_{\text{as}}(\text{CH}_3)$	
2919		$\nu_{\text{as}}(\text{CH}_2)$	
2872		$\nu_{\text{s}}(\text{CH}_2)$	
2845		$\nu_{\text{s}}(\text{CH}_2)$	
2731		?	
1664		$\nu(\text{C}=\text{C})$	Cornell and Koenig (1969); Hendra and Jackson (1994); Samran et al. (2004) Xue (1997); Taksapattanakul et al. (2017)
1642		$\nu(\text{C}=\text{CH}_2)$	Cornell and Koenig (1969)
1623		Dialkenyl sulfide crosslinks	Koenig et al. (1971); Hendra and Jackson (1994); Taksapattanakul et al. (2017)
1592		Conjugated trienes	Xue (1997); Taksapattanakul et al. (2017)
1573	1	?	
1554	2	?	
1526	3	?	
1506	4	?	
1488	5	?	
1458		$\nu_{\text{as}}(\text{CH}_3)$, $\delta(\text{CH}_2)$	Taksapattanakul et al. (2017)
1447		$\delta_{\text{as}}(\text{CH}_3)$	Cornell and Koenig (1969), Taksapattanakul et al. (2017)
1439		$\delta(\text{CH}_2)$, $\delta_{\text{s}}(\text{CH}_2)$	
1432		$\delta_{\text{s}}(\text{CH}_2)$	Samran et al. (2004)
1407		?	
1377*		$\nu(\text{C}=\text{C})$ $\delta_{\text{as}}(\text{CH}_3)$	Bunce et al. (1993) Cornell and Koenig (1969)
1363*		$\delta_{\text{as}}(\text{CH}_2)$, $\delta_{\text{a}}(\text{CH}_3)$	Taksapattanakul et al. (2017)
1343*		$\delta_{\text{s}}(\text{C}=\text{H})$ in-plane, $\delta_{\text{s}}(\text{CH}_3)$	Cornell and Koenig (1969); Haider (2012)
1315*		$\nu(\text{C}=\text{C})$ $\omega(\text{CH}_2)$	Bunce et al. (1993); Samran et al. (2004)
1301		?	Taksapattanakul et al. (2017)
1284*		$\delta(\text{C}=\text{H})$ in plane	Cornell and Koenig (1969); Bunce et al. (1993); Samran et al. (2004)
1214		$\delta(\text{C}=\text{H})$ in plane	Xue (1997)
1164		$\nu(\text{C}-\text{C})$	Cornell and Koenig (1969); Samran et al. (2004)
1069		?	
1038		$\gamma_{\text{r}}(\text{CH}_3)$	
1007		$\nu(\text{C}-\text{CH}_2)$	
992		?	
952		?	
733		$\nu(\text{C}-\text{S})$	Koenig et al. (1971)
721		$\nu(\text{C}-\text{S})$	
704		$\nu(\text{C}-\text{S})$	
682		$\nu(\text{C}-\text{S})$	
651		$\nu(\text{C}-\text{S})$	Hernández et al. (2016)
607	6	?	
597	7	?	
586	8	?	
570	9	?	
554	10	?	
540	11	?	

Table 1 (continued)

This study	No. (Fig. 2)	Assignment	References
515		$\nu(\text{S-S})$?	
505		$\nu(\text{S-S})$	Koenig et al. (1971); Hendra and Jackson (1994); Xue (1997); Hernández et al. (2016)
491		$\nu(\text{S-S})$ $\gamma(=\text{C-C}_2)$	
451		$\nu(\text{S-S})$	
434		$\nu(\text{S-S})$	
421		$\nu(\text{S-S})$? $\gamma(=\text{C-C}_2)$	

*Frequencies characteristic for *cis*-1,4 configuration after Bunce et al. (1993) and Haider (2012).

Abbreviations: ν : stretching (ν_s =symmetric; ν_{as} =asymmetric); δ : bending or deformation; γ_r : rocking; ω : twisting

occurs near 651 cm^{-1} that can be assigned to C-S stretching modes (Hernández et al. 2016). In addition, the upper

spectrum in Fig. 2 of the GMH LIX20 specimen shows two weak but resolvable bands at 733 and 721 cm^{-1} , presumably

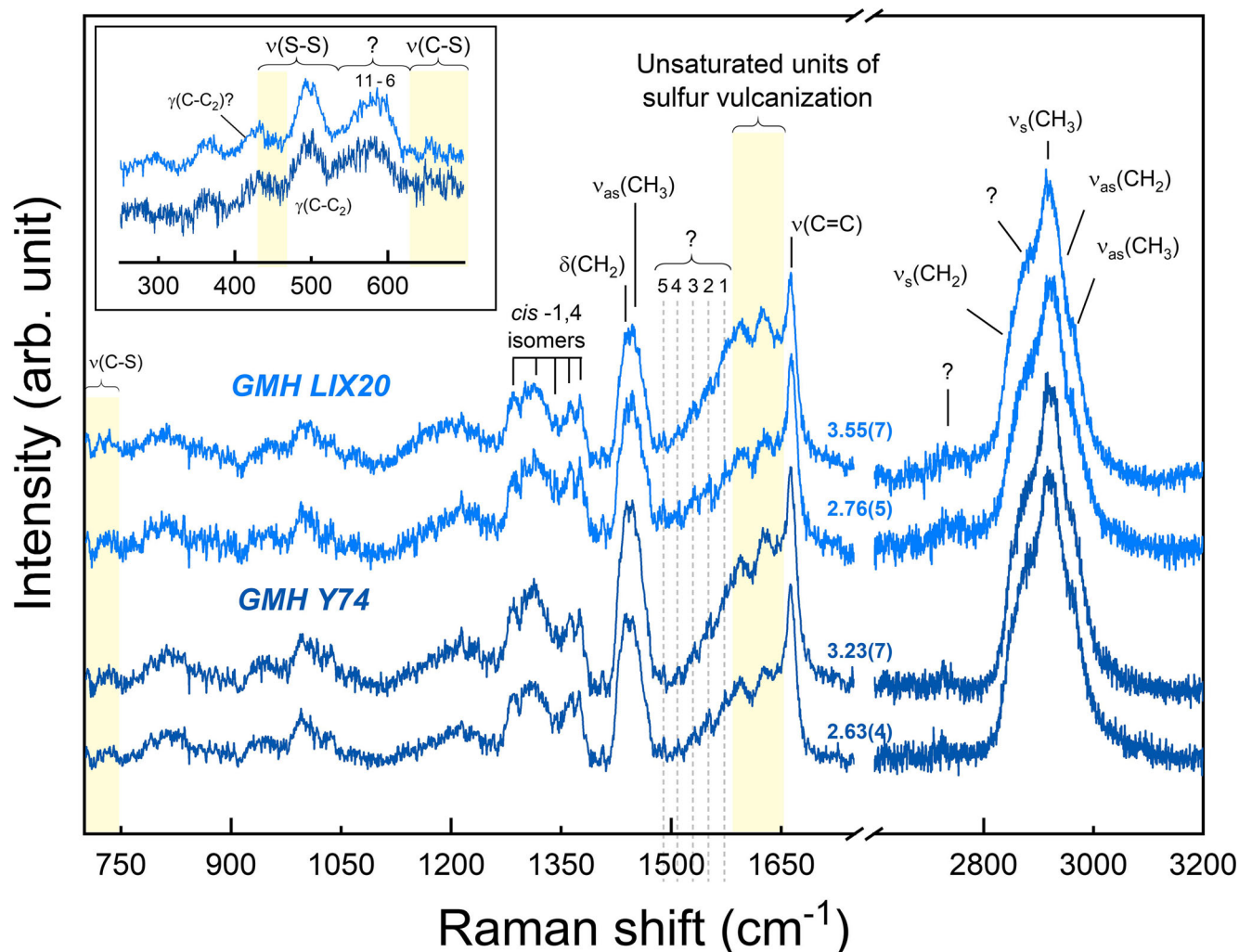


Fig. 2 Stacked plot of representative Raman spectra from the two laticifer specimens (GMH Y74 and GMH LIX20) in the frequency range between 250 and 700 (inset), 700 and 1700, and 2600 and 3200 cm^{-1} . The bands that can be assigned to sulfur species are highlighted with a yellow background, while those that cannot be assigned yet are labeled by numbers (cf. Table 1). Colored numbers at each sample spectrum

represent the ratio of the integrated intensity between 1480 and 1650, and 1650 and 1700 cm^{-1} . The number in parenthesis represents the propagated 2-sigma counting errors of the ratio and refers to the last digit. Note the significantly different ratios from different areas and samples, indicating a variable degree of vulcanization throughout the laticifers

representing symmetrical stretching modes of C-S bonds associated with dialkenyl sulfide cross-linkages (Koenig et al. 1971; Hernández et al. 2016). It is notable that these weak bands cannot be detected in all recorded spectra, again suggesting local differences in the degree of vulcanization process.

Natural rubber has a distinctive Raman spectrum that is unchanged by fossilization, except for the additional vulcanization bands. Moreover, the presence of S-S and C-S bonds as well as the main chain modification clearly indicate sulfur vulcanization. As already mentioned above, the spectral differences observed within one specimen may indicate different local conditions during the vulcanization processes which are presumably linked to local variations in sulfur concentration, since we can exclude large temperature fluctuations on the micrometer scale. Thus, it would have been desirable to quantify these modifications as a function of sulfur content or curing temperature and duration, for example, comparable to the systematic studies of Hendra and Jackson (1994) and Hernández et al. (2014, 2016). However, we would like to emphasize again that the presence and concentrations of these groups in the vulcanizate depend on different factors such as the relative ratios of sulfur to accelerator, the concentration of activators, and the time and temperature of vulcanization (Bateman et al. 1963). Thus, future research to calibrate the Raman spectra of vulcanized rubber produced through the low-temperature vulcanization of natural Apocynaceae latex under various temperature conditions is needed to be able to quantitatively interpret our results.

Fossilization at low temperatures

A representative, background-corrected Raman spectrum in the frequency range between 1000 and 1800 cm^{-1} from the black, carbonaceous material associated with the laticifers (Fig. 1b) is shown in Fig. 3. The raw spectrum is also shown in Fig. 3a with a linear background that accounts for the fluorescence caused by 532 nm excitation. Visible inspection of the Raman spectrum unambiguously indicates an immature, highly disordered, possible amorphous nature of the dark-carbonaceous material when compared to spectra obtained from material that experienced temperature in excess of 100 °C (cf. Fig. 4 of Rahl et al. 2005), which is clear evidence that the laticifers did not experience any high temperature event.

In the following, we discuss in greater detail the Raman spectra in regard to applying a geothermometer to low-temperature materials, as compared to applying the currently available thermometers. The expected maximum temperatures for the Geiseltal laticifers are outside the calibration range of all carbon geothermometers except one that was calibrated on extra-terrestrial carbon. Hence, currently, there are no available thermometers that can be directly used to determine the

maximum temperatures to which our specimens were subjected. However, by testing these models against the Raman spectra of the low-maturity material, we can evaluate which ones seem to be most accurate and thus most promising for further development in low-temperature geothermometry. These future models could then be utilized to determine the vulcanization temperatures for a wide variation of fossil latex.

The spectra are characterized by two very broad band profiles near 1580 and 1380 cm^{-1} . In graphite, the first band, the so-called G band, is due to the Raman-allowed E_{2g} vibrations of the carbon rings in the plane of the graphite sheets, while the second band, the so-called D (= D_1) band, reflects the A_{1g} breathing mode which is only allowed at the broken borders of graphene planes (e.g., Ferrari and Robertson 2000). The D band emerges as a result of structural disorder, whereas the G band becomes more intense with the increase of structural order and crystallite size until it is the only first order band in well-ordered graphite (e.g., Tuinstra and Koenig 1970; Ferrari and Robertson 2000; Pimenta et al. 2007). The thermal transition of carbonaceous matter to graphite as a function of temperature is well-reflected in the Raman spectrum. This has led to a number of Raman carbon geothermometers using different Raman band parameters, which was recently reviewed and discussed in great detail by Henry et al. (2019).

The first carbon geothermometer that we tested against the Geiseltal carbonaceous material is the only one that extends to temperatures below 100 °C (Homma et al. 2015); this was calibrated on carbonaceous material in chondrites and therefore cannot be directly applied to low-thermal-maturity, terrestrial, carbonaceous material. The lower limit of this thermometer is approximately 20–30 °C. Homma et al. (2015) fit the spectrum of their reference samples with four Gauss-Lorentz functions and found good correlation between maximum temperature and the band width of the D_1 band (given as full width at half maximum, FWHM). Using their fitting procedure (Fig. 3a) and their temperature versus FWHM(D_1) calibration, we obtain a temperature of 94 ± 39 °C from the Geiseltal carbonaceous material (Table 2). This relatively low temperature is fully consistent with the thermal history of the Geiseltal material, suggesting that a similar fitting procedure calibrated on terrestrial material may be an effective low-temperature geothermometer.

The second geothermometer that we applied to the Geiseltal carbonaceous material is that of Rahl et al. (2005). The lower limit of this carbonaceous material geothermometer is 100 °C, which is likely a higher temperature than the Geiseltal carbonaceous material was exposed to. We applied their method and calibration which is based on two intensity ratios (Table 2). With their fitting method (Fig. 3b) and calibration, we obtain a temperature of 291 ± 50 °C (Table 2). This temperature, however, does not match what is known of the thermal history of the Geiseltal site. Moreover, it does not

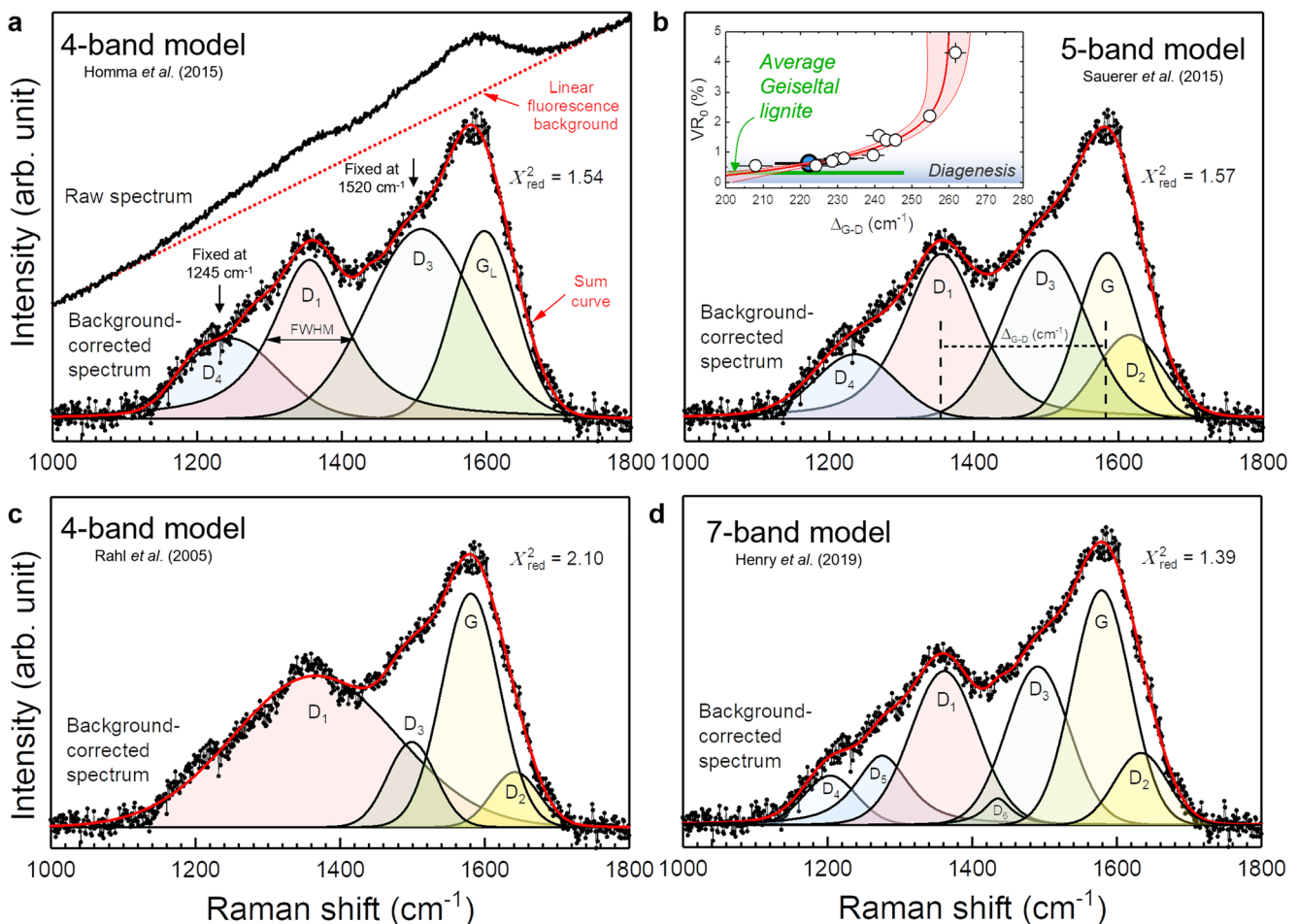


Fig. 3 Representative, fluorescence background-corrected Raman spectrum from carbonaceous bark material from the Geiseltal (Fig. 1c) surrounding the laticifers that was fit with different numbers of Gauss-Lorentz functions following the fitting procedures of various authors to extract quantitative information about the maximal coalification temperature of the bark material. **a** 4-band model of Homma et al. (2015), who fixed the D₃ and D₄ band during fitting at 1245 and 1520 cm⁻¹ and calibrated the width of the D₁ band (given as full width at half maximum, FWHM) of carbonaceous matter from chondrites against the expected peak temperature down to temperatures of 20 to

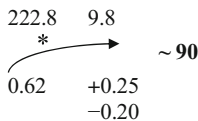
30 °C. **b** 4-band model of Rahl et al. (2005) used for carbonaceous matter that experienced peak temperatures greater 100 °C. **c** 5-band model of Sauerer et al. (2017), who reported a good correlation between the difference of the G and D₁ frequency, Δ_{G-D} , with the vitrinite reflectance. Inset shows a plot of vitrinite reflectance, VR_0 , as a function of Δ_{G-D} with the data of Sauerer et al. (2017) and an exponential fit with 95 % confidence interval from which we obtain a VR_0 value of 0.62 % for the carbonaceous bark material. **d** 7-band model of Henry et al. (2019) to fit highly immature carbonaceous matter. See text for more details

match at all the visual impression obtained by comparing the Raman spectra from the carbonaceous material surrounding the laticifers (Fig. 3) with those of carbonaceous material that has been heated to temperatures of 250 to 300 °C (cf. Fig. 4 of Rahl et al. 2005). This thermometer does not seem promising for application to low-temperature materials.

The third geothermometer we applied to the Geiseltal carbonaceous material involves an intermediate step of calculating the vitrinite reflectance from the Raman spectra. Sauerer et al. (2017) present a very good correlation ($r^2 = 0.95$) between the vitrinite reflectance of sedimentary carbonaceous matter (kerogen) of predominantly marine Type II and the separation of the D₁ and G band, Δ_{G-D} , in their Raman spectra. The vitrinite reflectance can, in turn, be used to infer the peak burial temperature (Burnham and

Sweeney 1989; Barker and Goldstein 1990). It is important to note that their Raman spectra were also excited with a 532 nm laser, as the Raman frequencies of carbonaceous matter strongly depend on the excitation wavelength (e.g., Pimenta et al. 2007; Sauerer et al. 2017). The authors fitted five Gauss-Lorentz bands to the first order Raman spectrum of the samples, as shown for the representative spectrum (Fig. 3c). In Fig. 3c, we have also replotted the data of Sauerer et al. (2017), as they do not report the fitting function, as well as fitted an exponential function of the form: $VR_0 = VR_0(0) + A \exp(B \Delta_{G-D})$ to the data and obtained $VR_0(0) = 262.0 \pm 4.1$, $A = -72.7 \pm 10.4$, and $B = -1.94 \pm 0.27$. From this calibration and the average Δ_{G-D} obtained for the fossil material, we obtain a vitrinite reflectance value of $VR_0 = 0.62^{+0.25}_{-0.20}$ % (Table 2). Although this value is

Table 2 Results of least-squares deconvolution of 57 Raman spectra from carbonaceous material from the Geiseltal monkeyhair using different fitting models to determine the maximum temperature of vulcanization (bold numbers)

Model	4-band model (Homma et al. 2015)				4-band model (Rahl et al. 2005)				5-band model (Sauerer et al. 2017)				7-band model (Henry et al. 2019)			
Bands [#] Parameters	ν (cm ⁻¹)	$\pm 1\sigma$	FWHM (cm ⁻¹)	$\pm 1\sigma$	ν (cm ⁻¹)	$\pm 1\sigma$	FWHM (cm ⁻¹)	$\pm 1\sigma$	ν (cm ⁻¹)	$\pm 1\sigma$	FWHM (cm ⁻¹)	$\pm 1\sigma$	ν (cm ⁻¹)	$\pm 1\sigma$	FWHM (cm ⁻¹)	$\pm 1\sigma$
D4	1245.0	<i>fixed</i>	152.3	11.1	-	-	-	-	1242.9	10.2	144.5	19.4	1205.7	10.5	93.1	24.7
D5	-	-	-	-	-	-	-	-	-	-	-	-	1274.3	7.4	88.5	26.6
D1	1356.6	3.7	139.2	5.7	1364.6	3.1	264.1	6.1	1358.4	4.3	134.1	11.9	1357.8	4.5	117.8	19.6
D6	-	-	-	-	-	-	-	-	-	-	-	-	1440.0	10.8	42.9	12.6
D3	1520.0	<i>fixed</i>	176.3	6.3	1495.3	2.9	76.4	7.9	1492.3	8.0	128.5	7.8	1491.6	2.4	124.9	33.3
G	1597.6	4.8	98.3	4.7	1576.5	4.4	96.2	2.1	1581.2	5.5	99.0	4.1	1576.8	2.6	97.2	9.9
D2	}				1632.9	3.6	86.2	2.5	1612.7	4.0	118.9	16.8	1629.4	11.9	77.4	16.3
R1 [§]					0.68	0.04										
R2 [§]					0.60	0.09										
Δ_{G-D} (cm ⁻¹)									222.8	9.8						
T (°C)	94	39			291	50										
VR ₀ (%)									0.62	+0.25	-0.20					

[#] The band nomenclature was taken from the publication given in the column label. * Estimated from the determined VR₀ value and from peak temperature *versus* VR₀ data of Barker and Pawlewicz (1986), Barker and Goldstein (1990), and Burnham and Sweeney (1989). [§] The ratios R1 and R2 are defined as R1 = [D₁/G]_H and R2 = [D₁/(G + D₁ + D₂)]_A, where the index H and A stands for the peak height and area, respectively.

significantly higher than the average VR₀ value of 0.277% measured for the Geiseltal lignite (Schmitz et al. 2001), it translates to a maximum temperature of less than ~ 90 °C (Barker and Pawlewicz 1986; Burnham and Sweeney 1989; Barker and Goldstein 1990). It is noteworthy that this estimate agrees well with the temperature of 94 ± 39 °C obtained from the geothermometer of Homma et al. (2015), although this thermometer was calibrated with inorganic carbonaceous matter from extraterrestrial sources. The temperature estimate obtained can thus be taken to suggest that the thermometer of Homma et al. (2015) also works in general for immature terrestrial carbonaceous material.

Finally, although there does not yet exist a complete and fundamental physical understanding of the Raman spectrum of low-maturity carbonaceous matter, Henry et al. (2019) suggest that Raman spectra from thermally highly immature carbonaceous samples/material should be fitted with seven Gauss-Lorentz functions to account for every visible local maximum in the spectra. Indeed, a 7-band fit to the Raman data from the fossil carbonaceous material yielded the lowest reduced X_{red}^2 of all fits (Fig. 3D and Table 2), but this is at least in part the effect of adding another fit function. Correlation between parameters of a seven-band fit and maximum temperature has not yet been developed, but this may also be a fruitful direction to developing a Raman geothermometer for low-thermal-maturity carbonaceous material.

In summary, visual examination alone of the Raman spectrum of the carbonaceous material associated with the laticifers provides evidence for a low degree of maturity (Fig. 3), which is typical for carbonaceous matter that has not experienced temperatures in excess of 100 °C. This also agrees well with the VR₀ value of 0.277 % that was previously measured for the Geiseltal lignite (Schmitz et al. 2001) and the lack of evidence for fires as a local heat source (Wilde and Riegel 2010). In quantitative terms, the low-thermal maturity of the fossil carbonaceous material is most clearly reflected by the geothermometer of Homma et al. (2015) which was calibrated for carbonaceous material from extra-terrestrial sources and yields a temperature of 94 ± 39 °C. Moreover, the VR₀ value of 0.62^{+0.25}_{-0.20} % that was indirectly determined from the Raman spectrum also corresponds to a maximum peak temperature of lower than ~ 90 °C (Barker and Pawlewicz 1986; Burnham and Sweeney 1989; Barker and Goldstein 1990). Both Raman geothermometers, as well as a new geothermometer based on a 7-band fit (Henry et al. 2019), are likely to work well, after further low-temperature calibration on low-thermal-maturity carbonaceous material. However, the origin of all seven or possibly even eight individual bands is not yet fully understood and may contain further information about the origin of the organic matter.

It is well-known that, besides temperature, the vulcanization process is also influenced by the sulfur source, accelerators, activators, and fillers (Mukhopadhyay et al. 1977;

Mukhopadhyay and De 1979; Coran 1994). We are not yet certain how these other factors contributed to the vulcanization of the Geiseltal laticifers (McCoy et al. 2021a), but the significant local variations of the relative intensity between sulfur- and rubber-related bands observed indicates that temperature alone did not control the vulcanization process or the physical properties, such as durability and elasticity, of the final product.

Conclusions

High-resolution analysis by Raman spectroscopy shows direct evidence that the latex of the laticiferous monkeyhair from the Eocene Geiseltal lignites are natural, sulfur-vulcanized *cis*-1,4-polyisoprene rubber, as identified by main chain modifications of natural latex and additional bands. It is thus concluded that sulfur was incorporated in the laticifers and does not occur exclusively as elementary sulfur. It follows that the vulcanization of the monkeyhair laticifers resulted as part of a natural sulfur vulcanization process. Moreover, the Raman spectrum of the carbonaceous material associated with the laticifers shows a low degree of maturity, which is typical for carbonaceous matter that has not experienced temperatures in excess of 100 °C. It is thus evident that the monkeyhair laticifers were not subjected to temperatures significantly higher than the surrounding coal.

This case study on Eocene latex and fossil laticifers demonstrates that Raman spectroscopy is a versatile and non-destructive analytical tool that can analyze fossil plants *in situ* for the presence of preserved latex without the need for any further sample preparation, thus avoiding any damage or modification of the original specimen. A targeted search for preserved latex in fossil plants from extant laticiferous lineages, as well as Raman spectroscopic assessment of any visually identified latex, would expand our knowledge of the fossil record and evolutionary history of latex. The development of new Raman geothermometers for low-thermal-maturity carbonaceous material would also help untangle the role of temperature in latex fossilization through vulcanization.

Supplementary Information The online version contains supplementary material available at <https://doi.org/10.1007/s12549-022-00566-8>.

Acknowledgments We thank Oliver Wings (former Curator at Martin-Luther-University, Halle-Wittenberg) for facilitating specimen access. George Mustoe and one anonymous reviewer are gratefully acknowledged for their constructive input. Funding was provided by DFG FOR 2685 grants to the University of Bonn for project numbers 396710782 to P. Martin Sander for M.I.L. and T.G., 396637283 to Jes Rust for V.E.M., 39676817 to C.T.G., and DFG INST 217 1010-1 to T.G. This is contribution no. 38 of the DFG Research Unit 2685, “The Limits of the Fossil Record: Analytical and Experimental Approaches to Fossilization.”

Funding Open Access funding enabled and organized by Projekt DEAL.

Data Availability The datasets generated during and/or analyzed during the current study are available from the corresponding author on reasonable request. This manuscript has not been published elsewhere, nor is it in review at another journal. All authors have reviewed and approve of the version submitted here.

Declarations

Conflict of interest The authors declare that they have no conflict of interest.

Open Access This article is licensed under a Creative Commons Attribution 4.0 International License, which permits use, sharing, adaptation, distribution and reproduction in any medium or format, as long as you give appropriate credit to the original author(s) and the source, provide a link to the Creative Commons licence, and indicate if changes were made. The images or other third party material in this article are included in the article's Creative Commons licence, unless indicated otherwise in a credit line to the material. If material is not included in the article's Creative Commons licence and your intended use is not permitted by statutory regulation or exceeds the permitted use, you will need to obtain permission directly from the copyright holder. To view a copy of this licence, visit <http://creativecommons.org/licenses/by/4.0/>.

References

- Agrawal, A. A., & Konno, K. (2009). Latex: A model for understanding mechanisms, ecology, and evolution of plant defense against herbivory. *Annual Review of Ecology, Evolution, and Systematics*, 40, 311–331.
- Alliger, G., & Sjöthun, I. J. (1964). *Vulcanization of Elastomers*. New York: Reinhold Publishing Corp.
- Baas, P., Manchester, S. R., Wheeler, E. A., & Srivastava, R. (2017). Fossil wood with dimorphic fibers from the Deccan Intertrappean Beds of India—The oldest fossil Connaraceae? *IAWA Journal*, 38, 124–133.
- Barker, C. E., & Pawlewicz, M. J. (1986). The correlation of vitrinite reflectance with maximum temperature in humic organic matter. In G. Buntbarth & L. Stegena (Eds.), *Paleogeothermics*, Lecture Notes in Earth Sciences, 5, pp. 115–129. Berlin, Heidelberg: Springer.
- Barker, C. E., & Goldstein, R. H. (1990). A fluid inclusion technique for determining maximum temperature in calcite and its comparison to the vitrinite reflectance geothermometer. *Geology*, 18, 1003–1006.
- Bateman, L., Moore, C. G., Porter, M., & Saville, B. (1963). Chemistry of vulcanisation. In L. Bateman (Ed.), *Chemistry and Physics of Rubberlike Substances* (xiv+784 pp. 168s). London, New York: Wiley.
- Beck-Mannagetta, P. (1964). Fossiler Kautschuk aus der Braunkohle des Lavanttales (Ostkarnten). *Neues Jahrbuch für Geologie und Paläontologie, Monatshefte*, 11, 655–659. Stuttgart.
- Bunce, S. J., Edwards, H. G. M., Johnson, A. F., Lewis, I. R., & Turner, P. H. (1993). Synthetic polyisoprenes studied by Fourier transform Raman spectroscopy. *Spectrochimica Acta Part A: Molecular Spectroscopy*, 49, 775–783.
- Burnham, A. K., & Sweeney, J. (1989). A chemical kinetic model of vitrinite maturation and reflectance. *Geochimica et Cosmochimica*, 53, 2649–2651. [https://doi.org/10.1016/0016-7037\(89\)90136-1](https://doi.org/10.1016/0016-7037(89)90136-1)

- Call, V., & Dilcher, D. (1997). The fossil record of *Eucommia* (Eucommiaceae) in North America. *American Journal of Botany*, 84, 798–814.
- Collins, L. W., Rohar, P. C., Veloski, G. A., Mahlberg, P. G., Haubould, H., & White, C. M. (1995). Identification of polycyclic hydrocarbons in fossilised latex from brown coal. *Polycyclic Aromatic Compounds*, 7, 223–230.
- Coran, A. Y. (1994). Vulcanisation. In J. E. Mark, B. Erman, & F. R. Eirich, (Eds.), *Science and Technology of Rubber* (2nd ed., pp. 339–385). Academic Press.
- Cornell, S. W., & Koenig, J. L. (1969). Raman spectra of polyisoprene rubbers. *Division of Polymer Science*, 2, 546–549.
- Datta, R. N., Hofstra, J. W., Geurts, F. A. J., & Talma, A. G. (1999). Polyisoprene Fourier transform Raman spectroscopy for characterization of natural rubber reversion and of antireversion agents. *Rubber Chemistry and Technology*, 72, 829–843.
- Dussourd, D. E. (2003). Chemical stimulants of leaf-trenching by cabbage loopers: Natural products, neurotransmitters, insecticides, and drugs. *Journal of Chemical Ecology*, 29, 2023–2047.
- Dussourd, D. E. (2017). Behavioral sabotage of plant defenses by insect folivores. *Annual Review of Entomology*, 62, 15–34.
- Dussourd, D. E., & Denno, R. F. (1994). Host range of generalist caterpillars: Trenching permits feeding on plants with secretory canals. *Ecology*, 75, 69–78.
- Eissmann, L. (2002). Tertiary geology of the Saale–Elbe Region. *Quaternary Science Reviews*, 21, 1245–1274.
- Ferrari, A., & Robertson, J. (2000). Interpretation of Raman spectra of disordered and amorphous carbon. *Physical Review B*, 61, 14095–14107.
- Franco, M. J. (2010). *Soroceaxylon entreriensis* gen. et sp. nov. (Moraceae) from the Itzaingó Formation (Pliocene–Pleistocene), Paraná river basin, Argentina. *Revista Mexicana de Ciencias Geológicas*, 27, 508–519.
- Geisler, T., & Menneken, M. (2021). Raman spectroscopy in fossilization research: Basic principles, applications in paleontology, and a case study on an *Acanthodia* fish spine. In C. T. Gee, V. E. McCoy, & P. M. Sander (Eds.), *Fossilization: The Material Nature of Ancient Plants and Animals in the Paleontological Record* (pp. 73–114). Baltimore: Johns Hopkins University Press.
- Gothan, W. (1924). Kautschuk in der Braunkohle. *Braunkohle*, 38, 713–715.
- Gothan, W. (1927). Ergänzungen zu den Beobachtungen über die fossilen Kautschukrinden der älteren Braunkohle. *Zentralblatt für Mineralogie, Geologie und Paläontologie, Abteilung B*, 6, 209–211.
- Gottwald, H. (1976). Die Bestimmung der ‘Kautschukhölzer’ und ‘Kautschukrinden’ aus der Braunkohle des Geiseltales. *Abhandlungen des Zentralen Geologischen Institutes*, 26, 283–289.
- Hagel, J. M., Yeung, E. C., & Facchini, P. J. (2008). Got milk? The secret life of laticifers. *Trends in Plant Science*, 13, 631–639.
- Haider, K. S. (2012). *Rubber soul—The investigation of rubber by vibrational spectroscopy*. M.Sc. thesis, Freie Universität Berlin, Humboldt Universität zu Berlin, Technische Universität Berlin, & Universität Potsdam.
- Hendra, P. J., & Jackson, K. D. O. (1994). Applications of Raman spectroscopy to the analysis of natural rubber. *Spectrochimica Acta*, 50, 1987–1997.
- Henry, D. G., Jarvis, I., Gillmore, G., Stephenson, M., & Emmings, J. F. (2018). Assessing low-maturity organic matter in shales using Raman spectroscopy: Effects of sample preparation and operating procedure. *International Journal of Coal Geology*, 191, 135–151.
- Henry, D. G., Jarvis, I., Gillmore, G., & Stephenson, M. (2019). Raman spectroscopy as a tool to determine the thermal maturity of organic matter: Application to sedimentary, metamorphic and structural geology. *Earth-Science Reviews*, 198, 102936.
- Hernández, M., Grande, A. M., Dierkes, W., Bijleveld, J., Van Der Zwaag, S., & García S. J., (2016). Turning vulcanised natural rubber into a self-healing polymer: Effect of the disulfide/polysulfide ratio. *American Chemical Society*, 4, 5776–5784.
- Hernández, M., Pflueger, F., Lopez-Tobar, E., Kruglik, S. G., Garcia-Ramos, J. V., Sanchez-Cortes, S., & Ghomi, M. (2014). Disulfide linkage Raman markers: A reconsideration attempt. *Journal of Raman Spectroscopy*, 45, 657–664.
- Hofmann, W. (1989). *Rubber Technology Handbook*. Hanser Publishers.
- Homma, Y., Kouketsu, Y., Kagi, H., Mikouchi, T., & Yabuta H. (2015). Raman spectroscopic thermometry of carbonaceous material in chondrites: Four-band fitting analysis and expansion of lower temperature limit. *Journal of Mineralogical and Petrological Sciences*, 110, 276–282.
- Jackson, K. D. O., Loadman, M. J. R., Jones, C. H., & Ellis G. (1990). Fourier transform Raman spectroscopy of elastomers: An overview. *Spectrochimica Acta*, 46, 217–226.
- Joseph, A. M., George, B., Madhusoodanan, K. N., & Alex, R. (2015). Current status of sulphur vulcanisation and devulcanisation chemistry: Process of vulcanisation. *Rubber Science*, 28, 82–119.
- Jurasky, K. A. (1928). Die Herkunft des fossilen Kautschuks (‘Affenhaar’) in der mitteldeutschen Braunkohle. *Braunkohle*, 27, 1130–1132.
- Jurasky, K. A. (1930). Einige mikroskopische Präparate von Kautschukgewächsen aus der eozänen Braunkohle Mitteldeutschlands. *Zeitschrift der Deutschen Geologischen Gesellschaft*, 82, 533.
- Kindscher, E. (1924). Über ein Vorkommen von Kautschuk in mitteldeutschen Braunkohlenlagern. *Berichte der Deutschen Chemischen Gesellschaft*, 57, 1152–1157.
- Kirchheimer, F. (1935). Bau und botanische Zugehörigkeit von Pflanzenresten aus deutschen Braunkohlen. *Botanische Jahrbücher für Systematik, Pflanzengeschichte und Pflanzengeographie*, 67, 37–122.
- Koenig, J. L., Coleman, M. M., Shelton, J. R., & Starmer, P. H. (1971). Raman spectrographic studies of the vulcanization of rubbers. I. Raman spectra of vulcanized rubbers. *Rubber Chemistry and Technology*, 44, 71–86.
- Konno, K. (2011). Plant latex and other exudates as plant defense systems: Roles of various defense chemicals and proteins contained therein. *Phytochemistry*, 72, 1510–1530.
- Krumbiegel, G. (1959). *Die tertiäre Pflanzen- und Tierwelt der Braunkohle des Geiseltales* Lutherstadt Wittenberg: A. Ziemsen Verlag.
- Krumbiegel, G., Rüffle, L., & Haubold, H. (1983). *Das eozäne Geiseltal: ein mitteleuropäisches Braunkohlenvorkommen und seine Pflanzen- und Tierwelt*. Lutherstadt Wittenberg: A. Ziemsen Verlag.
- Kvaček, Z., & Sakala, J. (1999). Twig with attached leaves, fruits and seeds of *Decodon* (Lythraceae) from the Lower Miocene of northern Bohemia, and implications for the identification of detached leaves and seeds. *Review of Palaeobotany and Palynology*, 107, 201–222.
- Mahlberg, P. G., & Störr, M. (1989). Fossil rubber in brown coal deposits: An overview. *Zeitschrift für Geologische Wissenschaften*, 17, 475–488.
- Mahlberg, P. G., Field, D. W., & Frye, J. S. (1984). Fossil laticifers from Eocene brown coal deposits of the Geiseltal. *American Journal of Botany*, 71, 1192–1200.
- Mathiesen, F. J. (1975). Palaeobotanical investigations into some cormophytic macrofossils from the Neogene Tertiary lignites of Central Jutland. III. Angiosperms. *Biologische Skrifter*, 20, 1–59.
- McCoy, V. E., Boom, A., Wings, O., Wappler, T., Labandeira, C. C., & Gee, C. T. (2021a). Fossilization of the Eocene “monkeyhair” laticifer tree from Geiseltal, Germany: A deeper understanding using micro-CT and pyrolysis GC/MS. *Palaos*, 36, 1–14.
- McCoy, V. E., Wappler, T., & Labandeira, C. C. (2021b). Exceptional fossilization of ecological interactions: Plant defenses during the four major expansions of arthropod herbivory in the fossil record. In C. T. Gee, V. E. McCoy, & P. M. Sander (Eds.), *Fossilization: The Material Nature of Ancient Plants and Animals in the*

- Paleontological Record* (pp. 187–220). Baltimore: Johns Hopkins University Press.
- McCoy, V. E., Gee, C. T., Michalski, J. M., & Wings, O. (2022). Oldest fossil evidence of latex sabotaging behavior by herbivorous insects. *Review of Palaeobotany and Palynology*, 300, 104631.
- Mukhopadhyay, R., & De, S.K. (1979). Effect of vulcanisation temperature and different fillers on the properties of efficiently vulcanised natural rubber. *Rubber Chemistry and Technology*, 52, 263–277.
- Mukhopadhyay, R., De, S. K., & Chakraborty, S. N. (1977). Effect of vulcanisation temperature and vulcanisation systems on the structure and properties of natural rubber vulcanizates. *Polymer*, 18, 1243–1249.
- Nallasamy, P., & Mohan, S. (2004). Vibrational spectra of cis-1,4-polyisoprene. *The Arabian Journal for Science and Engineering*, 29, 18–25.
- Pimenta, M., Dresselhaus, G., Dresselhaus, M. S., Cancado, L., Jorio, A., & Saito, R. (2007). Studying disorder in graphite-based systems by Raman spectroscopy. *Physical Chemistry Chemical Physics*, 9, 1276–1290.
- Rahl, J. M., Anderson, K. M., Bandon, M. T., & Fassoulas, C. (2005). Raman spectroscopic carbonaceous material thermometry of low-grade metamorphic rocks: Calibration and application to tectonic exhumation in Crete, Greece. *Earth and Planetary Science Letters*, 240, 339–354.
- Riegel, W., Bode, T., Hammer, J., Hammer-Schiemann, G., Lenz, O., & Wilde, V. (1999). The palaeoecology of the lower and middle Eocene at Helmstedt, northern Germany: A study in contrasts. *Acta Palaeobotanica Supplement*, 2, 349–358.
- Samran, J., Phinyocheep, P., Daniel, P., Derouet, D., & Buzaré, J-Y. (2004). Raman spectroscopic study of non-catalytic hydrogenation of unsaturated rubbers. *Journal of Raman Spectroscopy*, 35, 1073–1080.
- Sauerer, B., Craddock, P. R., AlJohani, M. D., Alsamadony, K. L., & Abdallah, W. (2017). Fast and accurate shale maturity determination by Raman spectroscopy measurement with minimal sample preparation. *International Journal of Coal Geology*, 173, 150–157.
- Schmitz, G., Gieren, B., & Littke, R. (2001). Vorläufige Ergebnisse geochemischer und petrographischer Untersuchungen an Braunkohlen aus dem Geiseltal (Sachsen-Anhalt, Deutschland). *Hallesches Jahrbuch für Geowissenschaften, Reihe B, Beiheft*, 13, 49–56.
- Simoneit, B. R. T., Otto, A., & Wilde, V. (2003). Novel phenolic biomarker triterpenoids of fossil laticifers in Eocene brown coal from Geiseltal, Germany. *Organic Geochemistry*, 34, 121–129.
- Taksapattanakul, K., Tulyapitak, T., Phinyocheep, P., Ruamcharoen, P., Ruamcharoen, J., Lagarde, F., & Daniel, P. (2017). The effect of percent hydrogenation and vulcanisation system on ozone stability of hydrogenated natural rubber vulcanizates using Raman spectroscopy. *Polymer Degradation and Stability*, 141, 58–68.
- Tuinstra, F., & Koenig, J. L. (1970). Raman spectrum of graphite. *The Journal of Chemical Physics*, 53, 1126–1130.
- Venkatachalam, P., Geetha, N., Sangeetha, P., & Thulaseedharan, A. (2013). Natural rubber producing plants: An overview. *African Journal of Biotechnology*, 12, 1297–1310.
- Wilde, V., & Riegel, W. (2010). ‘Affenhaar’ revisited—Facies context of in situ preserved latex from the Middle Eocene of Central Germany. *International Journal of Coal Geology*, 83, 182–194.
- Wilde, V., Kvaček, Z., & Bogner, J. (2005). Fossil leaves of the Araceae from the European Eocene and notes on other aroid fossils. *International Journal of Plant Sciences*, 166, 157–183.
- Xue, G. (1997). Fourier transform Raman spectroscopy and its application for the analysis of polymeric materials. *Progress in Polymer Science*, 22, 313–406.

Publisher's note Springer Nature remains neutral with regard to jurisdictional claims in published maps and institutional affiliations.